

Evaluation of IWV from the numerical weather prediction WRF model with PPP GNSS processing for Bulgaria

Tzvetan Simeonov^{1,a}, Dmitry Sidorov^{2,b}, Felix Norman Teferle², Georgi Milev³, and Guergana Guerova¹

¹Faculty of Physics, Sofia University "St. Kliment Ohridski", Bulgaria

^anow at GeoForschungsZentrum (GFZ) Potsdam, Germany

²Université du Luxembourg, Luxembourg

^bnow at Astronomical Institute University of Bern, Switzerland

³Space Research and Technology Center - Bulgarian Academy of Sciences, Bulgaria

Correspondence to: Tzvetan Simeonov (simeonov@phys.uni-sofia.bg)

Abstract. Global Navigation Satellite Systems (GNSS) ~~meteorology~~ Meteorology is an established operational service providing hourly updated GNSS tropospheric products to the National Meteorologic Services (NMS) in Europe. In the last decade through the ground-based GNSS network densification and new processing strategies like Precise Point Positioning (PPP), it has become possible to obtain sub-hourly tropospheric products for monitoring severe weather events. In this work one year (January - December 2013) of sub-hourly GNSS tropospheric products (Zenith Total Delay) are computed using the PPP strategy for seven stations in Bulgaria. In order to take advantage of the sub-hourly GNSS data to derive Integrated Water Vapour (IWV) surface pressure and temperature with similar temporal resolution is required. As the surface observations are on 3 hourly basis the first step is to compare the surface pressure and temperature from the numerical weather prediction model ~~Weather Forecasting and Research~~ Research and Forecasting (WRF) with observations at three synoptic stations in Bulgaria. The mean difference between the two data-sets for 1) surface pressure is less than 0.5 hPa and the correlation is over 0.989, 2) temperature the largest mean difference is 1.1° C and the correlation coefficient is over 0.957 and 3) IWV mean difference is in range between 0.1-1.1 mm. The evaluation of WRF on annual bases shows IWV underestimation between 0.5 and 1.5 mm at five stations and overestimation at Varna and Rozhen. Varna and Rozhen have also much smaller correlation 0.9 and 0.76. The study of the monthly IWV variation shows that at those locations the GNSS IWV has unexpected drop in April and March respectively. The reason for this drop is likely problems with station raw data. At the remaining 5 stations a very good agreement between GNSS and WRF is observed with high correlation during the cold part of 2013 i.e. March, October and December (0.95) and low correlation during the warm part of 2013 i.e. April to August (below 0.9). The diurnal cycle of the WRF model shows a dry bias in the range of 0.5-1.5 mm. Between 00 and 01 UTC the GNSS IWV tends to be ~~underestimate~~

IWV underestimated, which is likely due to the processing window used. The precipitation efficiency from GNSS and WRF show very good agreement on monthly bases with a maximum in May-June and minimum in August-September. The annual precipitation efficiency in 2013 at Lovech and Burgas is about 6 %.

1 Introduction

5 The atmospheric water vapour is a key element of the hydrological cycle and participates in precipitation formation, energy transfer and atmospheric stability. Water vapour has a relatively short lifetime in the atmosphere, from one week to ten days and its complex life cycle includes vertical and horizontal transport, mixing, condensation, precipitation and evaporation. Due to its high temporal and spatial variability atmospheric water vapour is very demanding to observe.

An established method for monitoring water vapour is the radiosonde. In Europe, the radiosonde network consists of 93
10 stations operated by the National Meteorological Services (NMS) under the EUMETNET-EUCOS project (euc, 2016). The radiosonde provide high vertical resolution data but due to its high cost is operated only one or two times per day at 00 UTC, at 12 UTC or 00 and 12 UTC, respectively. To monitor the high temporal and spatial water vapour variability a new method was developed in the early 1990s using the Global Positioning System (GPS) signal delay. The method was called "GPS meteorology" but with the development of other GNSS, for example Glonass and Galileo, was renamed to "GNSS meteorology". A
15 memorandum of understanding between E-GVAP (the EUMETSAT GNSS water vapour program) and EUPOS (the European Position determination System), which opens opportunities to use GNSS data for Bulgaria and South East Europe is in action since 2012.

Multi-technique Multi-technique comparisons (Ning et al., 2012; Buehler et al., 2012; Van Malderen et al., 2014) have demonstrated that GNSS meteorology derived Integrated Water Vapour (IWV) has a root mean square error in the range of
20 0.4-0.6 mm. A number of studies compare IWV from GNSS and Numerical Weather Prediction (NWP) models in Europe. A recent study by Keernik et al. (2014) found that the HIRLAM NWP model underestimates the IWV by 59 % for values below 12 mm, and overestimates by 6-10 % for values over 25 mm. A study of the COSMO model diurnal IWV cycle over Germany (Tomassini et al., 2002), reports a systematic IWV underestimation larger than 1 mm in the model analysis between 06 and 18 UTC. For Switzerland, Guerova et al. (2003) report a good agreement between model analysis and GNSS in winter but in
25 summer, a significant underestimation of IWV was found in the model, which is well correlated with significant overestimation of light precipitation. For both Germany and Switzerland a systematic underestimation of the diurnal IWV cycle between 6 and 21 UTC in both the model analysis and forecast is reported in Guerova and Tomassini (September 2003). For Poland, Wilgan et al. (2016) developed an integration model for estimating ZTD using WRF and reports good agreement between the ZTD estimation of WRF, compared to both GNSS and radiosonde measurements.

30 A recent development in GNSS processing is use of the Precise Point Positioning (PPP) strategy (Zumberge et al., 1997). In contrast to the Precise Network Positioning (PNP) strategy, PPP uses original data without differencing. Since 2013, the International GNSS Service (IGS, (Dow et al., 2009; Caissy et al., 2012)) provides ultra-fast or real-time precise satellite orbit and clock corrections in support of PPP processing (Douša and Vaclavovic, 2014; Li et al., 2014; Yuan et al., 2014;

Ahmed et al., 2014). The PPP strategy has the advantage of being computationally much more efficient than PNP and hence can provide estimates for large networks of stations with high temporal resolution (every 5 min). This cannot be achieved by the more conventional PNP strategy and sufficient IT infrastructure. These new generation GNSS products are yet to be fully compared with the state-of-the-art NWP models and are of particular interest for very short range weather forecasting of severe weather events (nowcasting).

Use of GNSS derived Water Vapour (WV) in Europe is a well established techniques but there exist a large difference on regional level (Guerova et al., 2016) . While in West and central Europe the topic has reached maturity in South and particularly South-east Europe it is currently under development. During the last 5 years GNSS meteorology was developed in Bulgaria within a Marie Curie funded project. As apart a part of this project a regional database for Bulgaria and Southeast Europe the Sofia University Atmospheric Data Archive (SUADA, Guerova et al. (2014)) was developed to facilitate the use of GNSS tropospheric products (see Sect. 2.2). In this study for the first time a PPP GNSS processing strategy is applied to seven stations in Bulgaria and GNSS IWV is derived using the Weather ~~Forecasting System~~ Research and Forecasting (WRF) NWP model. The aim of this work is to evaluate the IWV from GNSS and the WRF NWP model for Bulgaria in 2013. The objectives are to: (1) derive GNSS IWV for Bulgaria using surface pressure and temperature from synop observations and the WRF model, (2) evaluate the WRF model IWV a) on annual and monthly basis and b) the diurnal cycle and (3) evaluate the ~~precipitation efficiency~~ Precipitation Efficiency (PE) (Bordi et al., 2015) of the WRF model for Bulgaria in 2013. In Section 2 are presented the GNSS processing strategy and the WRF model set up as well as the data-sets used. Section 3 presents the IWV annual and monthly comparison as well as the diurnal IWV cycle in GNSS and WRF. The summary and conclusions are given in Section 4.

2 Data sets and method

2.1 Numerical weather prediction model WRF set up

The WRF model is developed in the USA by a collaboration of groups at National Center for Atmospheric Research (NCAR), Mesoscale and Microscale Meteorology Division, the National Oceanic and Atmospheric Administration (NOAA), National Center for Environmental Prediction (NCEP), Earth System Research Laboratory (ESRL), Department of Defence Air Force Weather Agency (AFWA), Naval Research Laboratory (NRL), Center for Analysis and Prediction of Storms (CAPS), Federal Aviation Administration (FAA) and the University of Oklahoma. In this work the WRF v3.4.1 (~~NCAR, 2016~~) (NCAR, 2016; Skamarock et al., 2008) computed for a domain covering Bulgaria with a horizontal resolution of 9 km and a vertical resolution of 44 levels. The following parametrizations schemes for the model physics are selected: 1) Unified Noah land-surface model for the land surface (Chen et al., 1996), 2) Yonsei University (YSU) scheme for the planetary boundary layer (Hong et al., 2006), 3) WRF Single moment Microphysics (WSM) 6-class graupel scheme for the microphysics (Hong and Lim, 2006) and 4) Rapid Radiative Transfer Model (RRTM) for the long/short-wave radiation (Mlawer et al., 1997).

The WRF model output is integrated into the SUADA. Two types of WRF model parameters are archived in SUADA, namely surface parameters (pressure and temperature) and profiles (pressure, temperature, water vapour mixing ratio and the model

level height). Presented in Fig. 1 is the SUADA data flow. The surface parameters from WRF are archived in the NWP

SUBSCRIPTNBININ

SUBSCRIPTNBID-1D SUADA table and used to compute the GNSS IWV (Sect. 2.2). The profiles from WRF are archived in the NWP

5 SUBSCRIPTNBININ

SUBSCRIPTNB3D-3D SUADA table and are used to compute the water vapour density at each model level ($\rho_{wv}(z)$) and then by integration over the model levels the WRF-IWV is obtained as below:

$$IWV = \frac{1}{\rho_w} \int_z^{z_n} \rho_{wv}(z) dz \quad (1)$$

where ρ_w is density of liquid water, n is the number of model levels.

10 2.2 GNSS processing strategy and tropospheric products

Archived in SUADA are GNSS tropospheric products like Zenith Total Delay (ZTD over 12 000 000 individual observations) and derivatives like IWV (over 55 000) from five GNSS processing strategies and 37 stations in Bulgaria/Southeast Europe for the period 1997-2013. The temporal resolution of the GNSS data is from 5 minutes to 6 hours.

In this work we use GNSS tropospheric products from the BULgarian ~~intelegent~~-intelligent Positioning System (BULi-
15 POS, <http://www.bulipos.eu/> (2016)) GNSS network in Bulgaria. The BULiPOS network of reference stations was established in 2008 and has 26 stations mainly used for navigation and geodetic applications. ~~BULIPOS~~-BULiPOS provided Receiver Independent Exchange Format (RINEX) GNSS data for seven station for 2013 (Fig. 2). The GNSS tropospheric products (Zenith Total Delay, ZTD) were computed with the NAvigation Package for Earth Observation Satellites (NAPEOS, <http://www.positim.com/napeos.html> (2016)) software. NAPEOS is developed and maintained by the European Space Operations Centre (ESOC) of the European Space Agency (ESA). NAPEOS is used at ESOC since January 2008. The NAPEOS
20 version 3.3.1 was used for the processing in this study. The processing was performed at the University of Luxembourg using the GMF (Global Mapping Function) (Boehm et al., 2006) and 10° elevation cut-off angle. The data were processed using the PPP strategy employing IGS satellite orbits and clocks. The computed ZTDs are with a temporal resolution of 300 s (5 min).

The ZTD data is archived in the GNSS

25 SUBSCRIPTNBIN-IN SUADA table (Fig. 1). To derive GNSS-IWV the WRF model surface pressure (p_s , [hPa]) and temperature (t_s , [K]) are used in Eq. 2 (Davis et al., 1985) and Eq. 3,4 (Bevis et al., 1992)

$$ZWD = ZTD - 0.0022768 \frac{p_s}{1 - 0.00266 \cos(2\theta) - 0.00028h} \quad (2)$$

$$IWV = \frac{10^6}{(k_3/T_m + k'_2)R_v} ZWD, \quad (3)$$

$$T_m = 70.2 + 0.72t_s, \quad (4)$$

5 where $k'_2 = (17 \pm 10)[K^*hPa^{-1}]$, $k_3 = (3.776 \pm 0.004) * 10^5 [K^2*hPa^{-1}]$ are constants derived first by Thayer (1974) and $R_v = 461.51[J*kg^{-1}K^{-1}]$ is the gas constant for water vapour, T_m [K] is the weighted mean atmospheric temperature, h [km] is the height and θ is the latitude variation of the gravitational acceleration.

The pressure at the GNSS station altitude is calculated using the model pressure at the nearest model grid point. The pressure difference between the GNSS station altitude and the nearest NWP model grid point is calculated using the polytropic
10 barometric formula Sissenwine et al. (1962):

$$P_g = P_m \left(\frac{T}{T - L(H_g - H_m)} \right)^{\left(\frac{g_0 M_0}{R * L} \right)} \quad (5)$$

where P_g is the pressure at the GNSS station altitude, P_m is the pressure at meteorological station altitude, T [K] is the temperature in meteorological station, $L = 6.5 K/km$ is tropospheric lapse rate, H_m [km] is the altitude of the meteorological station, H_g [km] is the altitude of the GNSS station, $g_0 = 9.806 \frac{m}{s^2}$ is the gravitational acceleration, $M_0 = 28.9644 \frac{g}{mol}$ is the
15 molar mass of air and $R = 8.31432 \frac{Nm}{(molK)}$ is the universal gas constant.

2.3 Surface observations

Archived in SUADA are also surface observations of: 1) pressure, 2) 2 m temperature and 3) precipitation (PP). The measurements are from the surface observation network (SYNOP) of the National Institute of Meteorology and Hydrology (NIMH) in Bulgaria and are collected manually every 3 hours (00, 03, 06, 09, 12, 15, 18 and 21 UTC). The data is available from the
20 OGIMET weather information server (ogi, 2016). The surface pressure and temperature are used for derivation of IWV from the GNSS tropospheric products as described in Sect. 2.2. Using surface observations the IWV is derived every 3 hours and is referred to as IWV* in Table 1.

2.4 Precipitation efficiency

~~In order to study water availability Tuller (1971) proposed~~ The Precipitation Efficiency (PE) is a value, calculated for each station, which is descriptive for air masses in two time scales: Cloud Microphysics Precipitation Efficiency (CMPE) (Braham Jr, 1952) and Large-Scale Precipitation Efficiency (LSPE) Tuller (1971) . In this study we are assessing LSPE, which is representative for the
25

region climate and climate variations. PE is expressed as percentage of the IWV that is converted and measured as precipitation. Bordi et al. (2015) proposed to use GNSS IWV to compute PE. In this work the daily PE is computed as following:

$$PE = \frac{PP}{IWV} \cdot 100 \quad (6)$$

where PP and IWV are daily averaged precipitation and IWV at the station. Below Precipitation efficiency gives a long-term indication of stability of the atmosphere. In this study the two analysed stations for PE are in low altitudes; PE computed from GNSS IWV and observed PP is entitled GNSS PE and from WRF IWV and PP is entitled WRF PE.

3 Evaluation of the WRF model IWV with GNSS-IWV for 2013

3.1 Evaluation of WRF model surface pressure and temperature

The annual mean, standard deviation and correlation between the surface pressure and temperature from WRF and SYNOP are presented in Table 1. The WRF pressure and temperature are extracted with the temporal resolution of the SYNOP i.e. every 3 hours. The correlation coefficient between the two data sets for atmospheric pressure for station Lovech (LOVE) is 0.99 with the mean difference 0.5 hPa. The correlation coefficient for the temperature is 0.96. The largest differences in the two data sets are observed for December 2013. For station Varna (VARN) the correlation coefficient for the pressure is 1 and for the temperature 0.96 with a mean difference between the SYNOP and NWP-WRF of 0.2 hPa for the pressure and 0.2° C for the temperature. For station Burgas (BURG) the correlation coefficient for the pressure is 1 and for the temperature 0.96. The mean difference for the pressure is 0.1 hPa and 0.2° C for the temperature. The NWP-WRF surface pressure shows an agreement of 0.5 hPa or better with the SYNOP data-set. This allows to take advantage of deriving IWV with the temporal resolution of the GNSS tropospheric products. A comparison between IWV and IWV* for station Burgas is seen in Fig. 3.

3.2 WRF-GNSS IWV: annual and monthly mean

A comparison between the GNSS and WRF IWV is presented in Table 3. For Burgas, Lovech, Montana, Shumen and Stara Zagora the correlation coefficient is very high and lies between 0.95 and 0.96. The mean IWV difference is between 0.5 and 1.8 mm. The smallest mean difference is obtained for Shumen and Burgas and is a consequence of the small altitude difference between GNSS station and WRF model height (Table 2). The altitude difference for station Lovech is 107 m and there the largest mean difference of 1.8 mm is obtained. For Varna and Rozhen the correlation coefficient is 0.9 and 0.76, and the mean IWV difference is negative with -0.9 and -3.2 mm respectively.

The comparison between the GNSS and WRF monthly mean IWV for 2013 is presented in Fig. 4. At all stations with exception of Rozhen the monthly mean IWV minimum is 10 mm in December 2013 and the maximum is 25 mm in in June 2013. The GNSS and WRF IWV for station Burgas is shown in Fig. 4a. It can be seen that there is good agreement between the monthly mean IWV from GNSS and WRF. The correlation coefficient varies between 0.96 and 0.84. The maximum and

minimum correlation is seen in winter and autumn, and spring and summer, respectively. Between stations Shumen (Fig. 4b) and Stara Zagora (Fig. 4c) similarities in the IWV can be observed. The values indicate again a maximum in June and a minimum in December. For Shumen the lowest correlation is observed in April and it stays low during the spring months. For Stara Zagora the correlation coefficient stays low in with minimum from April till August. Montana (Fig. 4d) is in Northwest Bulgaria where the influence of the Balkan mountains is significant and the interaction with synoptic flows plays a major role for the IWV distribution. The lowest GNSS and WRF IWV values are seen for December 12 mm and the highest for June with 27 mm. For Varna (Fig. 4e) of interest is the difference between GNSS and WRF, which is seen during the months April and May. From January to April the IWV in the WRF is lower than the GNSS and from May to December it is the opposite. Similar GNSS IWV jump between April and May is seen at Rozhen (Fig. 4f). A possible reason for these changes is the GNSS station set up which needs further investigation.

Further work was carried out to investigate the possible reasons for reported drop in GNSS-IWV values at station Varna and Rozhen. The manual investigation of the raw GNSS data showed that at station Varna wrong antenna model as reported in the raw data. After the antenna model correction the processing resulted to an IWV increase by 2 mm in December 2013. For station Rozhen the manual investigation did not show any mistakes thus the problem remains there.

The datasets of Lovech and Shumen have the shortest gaps among the studied stations. These two stations were detrended using the following annual fitting function, as proposed by Ning (2012):

$$y = at + b\cos(2\pi t) + c\sin(2\pi t) + d\cos(4\pi t) + e\sin(4\pi t) \quad (7)$$

where b and c are the annual coefficients and d and e - the semi-annual, while a is a linear trend component. These coefficients were determined using least-square analysis. The correlation between the datasets is high (0.913 for Lovech and 0.901 for Shumen) after subtracting the seasonal variation (Fig. 7). This analysis could not be performed for the other 5 stations, because of the gaps in the datasets, which influence the trend analysis of both the annual variation and the monthly change in IWV.

3.3 WRF-GNSS IWV: diurnal cycle

In Fig. 5 half hourly IWV from GNSS and WRF are averaged and plotted for each station. The diurnal cycle of IWV for Burgas is presented in Fig. 5a. The WRF IWV is between 0.5 and 1.0 mm lower than for GNSS. The mean difference between the two data sets is around 0.5 mm up to 10 UTC. Between 10 and 20 UTC the difference is larger at around 1 mm. At Lovech (Fig. 5b) the difference between GNSS and WRF IWV is between 1.0 and 1.5 mm. This however is expected and is due to the discussed altitude difference (107 m) between the WRF grid point and the GNSS station. It is to be noted that the GNSS, WRF altitude difference is under 40 m for the other 4 stations. For Montana, Shumen and Stara Zagora WRF has a dry bias relative to the GNSS. For Montana (Fig. 5c) the estimated difference is between 1.2 and 1.7 mm. Larger differences between datasets are seen in the afternoon after 13 UTC (top plots in Fig. 5c). The mean difference in the diurnal IWV variation at Shumen (Fig. 5d) and Stara Zagora (Fig. 5e) between GNSS IWV and WRF IWV is in the range of 0.5 - 1.0 mm. At all stations between 00 and 01 UTC the GNSS has a tendency to underestimate IWV which is likely related to the limits of the beginning and the end

of the GNSS processing, called processing window. In the beginning of each processing the GNSS solution is unstable due to lack of initial conditions. The PPP processing uses daily IGS orbits files with jumps in the orbits on the day boundaries. These jumps influence the IWV values.

5 The WRF model has an underestimation of diurnal IWV cycle at all stations in the range of 0.5-1.5 mm Guerova and Tomassini (September 2016). It is not possible to link our study with the one done with COSMO model as each NWP model has its own characteristics (Guerova et al., 2016). NWP models are set up differently, and have different performance, depending on selected region, resolution, season and parametrisation schemes. Our experience with simulation of intense summer precipitation in Bulgaria during 2012 has shown that the WRF model has high sensitivity to the convective parameterisation scheme used and this prompted the present study to a full year check of the the model performance of the selected set-up.

3.4 WRF-GNSS comparison: precipitation efficiency in 2013

Figure 6 shows the monthly mean precipitation efficiency computed with GNSS and WRF for Burgas and Lovech. The very good agreement between the model and GNSS is apparent at both locations. At Burgas (Fig. 6a) the PE has minimum in August less than 1 % and maximum in May 14 %. For Lovech (Fig. 6b) the maximum PE is in May but is slightly smaller than in Burgas (12 %) and the minimum is in September of about 1 %. The PE at the two stations also shows differences with are expected as the two stations are located in different climatic regions in Bulgaria. While Burgas is in south-east Bulgaria close to the Black Sea, Lovech is in north-west Bulgaria. The atmospheric circulation in Bulgaria is dependent on the Balkan mountains in middle of the country i.e. south of the range the Mediterranean cyclones are the main source of precipitation, while the north of the range their influence is largely reduced. The annual PE in both stations is in the range of 5.5-5.8 % from GNSS and 5.9-6.0 % from WRF, which is in agreement with the range of 5-10 % for the region found in Tuller (1971).

4 Conclusions

In this work GNSS tropospheric products (ZTD) with temporal resolution 5 min are derived using the PPP processing for one year period. In order to take advantage of the high temporal resolution of GNSS products for derivation of IWV the surface pressure and temperature from the NWP WRF model is used. The WRF surface pressure and temperature was evaluated against surface observations from three synoptic stations in Bulgaria. The mean difference for surface pressure between the two data-sets is less than 0.5 hPa and the correlation is over 0.989. For the temperature the largest mean difference is 1.1° C and the correlation coefficient is over 0.957. The IWV computed with this two data-sets has a mean difference is in range of 0.1-1.1 mm.

The evaluation of WRF on annual bases shows IWV underestimation between 0.5 and 1.5 mm at five stations and overestimation at Varna and Rozhen. Varna and Rozhen have also much smaller correlation 0.9 and 0.76. The study of the monthly IWV variation shows that at those locations the GNSS IWV has unexpected drop in April and March, respectfully. The reason for this drop is likely problems with station raw data. At the remaining 5 stations a very good agreement between the GNSS

and WRF is observed with highest correlation in the cold part of the year i.e. March, October and December (over 0.95) and lowest correlation during the warm part of the year i.e. April to August (below 0.9). ~~The diurnal~~

The diurnal IWV cycle is investigated for Bulgaria for 2013. The diurnal variations of atmospheric water vapour affect long wave radiation, absorption of solar radiation and is related to processes such as atmospheric stability, diurnal variation of moist
5 convection and precipitation, surface wind convergence and evapotranspiration. Thus it is important to evaluate the IWV cycle
of the WRF model ~~shows for Bulgaria. At all stations the models has~~ a dry bias in the range 0.5-1.5 mm. ~~Between 00 and 01~~
~~UTC the GNSS IWV tends to be underestimated IWV, which is likely due to the processing time window used.~~ Studies with
other models show a link between IWV underestimation and overestimation of light precipitation. Such study could not be
performed for Bulgaria as the precipitation observations are only available as accumulated 6 hourly values.

10 In order to link the IWV and precipitation the precipitation efficiency coefficient is computed at two stations. Precipitation
efficiency gives the percentage of IWV converted in precipitation. The precipitation efficiency from GNSS and WRF show very
good agreement on monthly bases with a maximum in May-June and minimum in August-September. The annual precipitation
efficiency in 2013 at Lovech and Burgas is about 6 %, which is within the typical values range for low elevation stations in
moderate and continental climates. It will be interesting to investigate the precipitation efficiency at the mountainous stations
15 but co-location of GNSS and reliable surface observations is a limiting factor for such analysis.

This work is a first step of setting up GNSS Analysis Centre for tropospheric products at Sofia University (Sofia University
GNSS Analysis Centre - SUGAC). SUGAC is a collaboration between Sofia University and Space Research and Technology
Institute of the Bulgarian Academy of Sciences. The consistent PPP processing of 7 GNSS station demonstrates a potential to
provide IWV with high temporal resolution for validation of the state-of-the-art NWP models. However, operational provision
20 of GNSS tropospheric products is delayed due to the availability of real time RINEX data. The team at Sofia University is
working towards establishment of dedicate GNSS network for atmospheric remote sensing products in Bulgaria.

Acknowledgements. Tzvetan Simeonov ~~acknowledge~~ acknowledges the support provided by COST - European Cooperation in Science
and Technology project "Advanced Global Navigation Satellite Systems tropospheric products for monitoring severe weather events and
climate" (GNSS4SWEC) for Short-Term Scientific Mission (STSM) to University of Luxembourg. This work is supported by a Marie
25 Curie International Reintegration Grant (FP7-PEOPLE-2010-RG) within the 7th European Community Framework Programme and Sofia
University grant. The technical support by Dr. Stoyan Pisov and Dr. Elisaveta Peneva is greatly appreciated.

References

- EUCOS upper-air network, <http://www.eumetnet.eu/radiosonde-stations>, accessed: 2016-01-18, 2016.
- Ogimet Weather Information Service, <http://www.ogimet.com>, accessed: 2016-01-18, 2016.
- Ahmed, F., Vaclavovic, P., Teferle, F. N., Douša, J., Bingley, R., and Laurichesse, D.: Comparative analysis of real-time precise point positioning zenith total delay estimates, *GPS Solutions*, pp. 1–13, 2014.
- Bevis, M., Businger, S., Herring, T. A., Rocken, C., Anthes, R. A., and Ware, R. H.: GPS Meteorology: Remote Sensing of Atmospheric Water Vapour Using the Global Positioning System, *J. Geophys. Res.*, 97, 15 787–15 801, 1992.
- Boehm, J., Niell, A., Tregoning, P., and Schuh, H.: Global Mapping Function (GMF): A new empirical mapping function based on numerical weather model data, *Geophysical Research Letters*, vol.33, issue 7, doi: 10.1029/2005GL025546, 2006.
- 10 Bordi, I., Raziqi, T., Pereira, L. S., and Sutera, A.: Ground-based GPS measurements of precipitable water vapor and their usefulness for hydrological applications, *Water Resources Management*, 29, 471–486, 2015.
- Braham Jr, R. R.: The water and energy budgets of the thunderstorm and their relation to thunderstorm development, *Journal of Meteorology*, 9, 227–242, 1952.
- Buehler, S., Östman, S., Melsheimer, C., Holl, G., Eliasson, S., John, V., Blumenstock, T., Hase, F., Elgered, G., Raffalski, U., et al.: A multi-instrument comparison of integrated water vapour measurements at a high latitude site, *Atmospheric Chemistry and Physics*, 12, 10925–10943, 2012.
- 15 Caissy, M., Agrotis, L., Weber, G., Hernandez-Pajares, M., and Hugentobler, U.: Innovation: Comming Soon: The International GNSS Real-Time Service, *GPS World*, 23, 52, 2012.
- Chen, F., Mitchell, K., Schaake, J., Xue, Y., Pan, H.-L., Koren, V., Duan, Q. Y., Ek, M., and Betts, A.: Modeling of land surface evaporation by four schemes and comparison with FIFE observations, *Journal of Geophysical Research. D. Atmospheres*, 101, 7251–7268, 1996.
- 20 Davis, J., Herring, T., Shapiro, I., Rogers, A., and Elgered, G.: Geodesy by radio interferometry: Effects of atmospheric modeling errors on estimates of baseline length, *Radio science*, 20, 1593–1607, 1985.
- Douša, J. and Vaclavovic, P.: Real-time zenith tropospheric delays in support of numerical weather prediction applications, *Adv. Space Res.*, 53, 1347–1358, doi:10.1016/j.asr.2014.02.021, 2014.
- 25 Dow, J. M., Neilan, R. E., and Rizos, C.: The International GNSS Service in a Changing Landscape of Global Navigation Satellite Systems, *J. Geod.*, 83, 191–198, doi:10.1007/s00190-008-0300-3, 2009.
- Guerova, G. and Tomassini, M.: Monitoring IWV from GPS and limited - area forecast model, Tech. Rep. 2003-15, University of Bern, Switzerland, September 2003.
- Guerova, G., Brockmann, E., Quiby, J., Schubiger, F., and Matzler, C.: Validation of NWP mesoscale models with Swiss GPS Network AGNES, *Journal of Applied Meteorology*, 42, 141–150, 2003.
- 30 Guerova, G., Simeonov, T., and Yordanova, N.: Sofia University Atmospheric Data Archive (SUADA), *AMT*, 7, 2683–2694, doi:10.5194/amt-7-2683-2014, <http://www.atmos-meas-tech.net/7/2683/2014/>, 2014.
- Guerova, G., Jones, J., Douša, J., Dick, G., de Haan, S., Pottiaux, E., Bock, O., Pacione, R., Elgered, G., Vedel, H., and Bender, M.: Review of the state of the art and future prospects of the ground-based GNSS meteorology in Europe, *Atmospheric Measurement Techniques*, 9, 5385–5406, doi:10.5194/amt-9-5385-2016, <http://www.atmos-meas-tech.net/9/5385/2016/>, 2016.
- 35 Hong, S.-Y. and Lim, J.-O. J.: The WRF single-moment 6-class microphysics scheme (WSM6), *Asia-Pacific Journal of Atmospheric Sciences*, 42, 129–151, 2006.

- Hong, S.-Y., Noh, Y., and Dudhia, J.: A new vertical diffusion package with an explicit treatment of entrainment processes, *Monthly Weather Review*, 134, 2318–2341, 2006.
- <http://www.bulipos.eu/>: BULgarian Intelegent POSition determination System, <http://www.bulipos.eu/>, accessed: 2016-01-18, 2016.
- <http://www.positim.com/napeos.html>: NAPEOS software for processing GNSS data, <http://www.positim.com/napeos.html>, accessed: 2016-01-18, 2016.
- 5 Keernik, H., Ohvrila, H., Jakobsona, E., Rannata, and Luhamaa, A.: Column water vapour: an intertechnique comparison of estimation methods in Estonia, *Proceedings of the Estonian Academy of Sciences*, 63, 37–47, 2014.
- Li, M., Li, W., Shi, C., Zhao, Q., Su, X., Qu, L., and Liu, Z.: Assessment of Precipitable Water Vapor Derived from Ground-based BeiDou Observations with Precise Point Positioning Approach, *Adv. Space Res.*, doi:10.1016/j.asr.2014.10.010, 2014.
- 10 Mlawer, E. J., Taubman, S. J., Brown, P. D., Iacono, M. J., and Clough, S. A.: Radiative transfer for inhomogeneous atmospheres: RRTM, a validated correlated-k model for the longwave, *Journal of Geophysical Research: Atmospheres*, 102, 16 663–16 682, doi:10.1029/97JD00237, <http://dx.doi.org/10.1029/97JD00237>, 1997.
- NCAR, N.: Weather and Research Forecasting model, <http://www.wrf-model.org/index.php>, accessed: 2016-01-18, 2016.
- Ning, T.: GPS meteorology: with focus on climate application, Chalmers University of Technology, 2012.
- 15 Ning, T., Haas, R., Elgered, G., and Willén, U.: Multi-technique comparisons of 10 years of wet delay estimates on the west coast of Sweden, *Journal of Geodesy*, 86, 565–575, 2012.
- Sissenwine, N., Dubin, M., and Wexler, H.: The U.S. Standard Atmosphere, 1962, *Journal of Geophysical Research*, 67, 3627–3630, doi:10.1029/JZ067i009p03627, <http://dx.doi.org/10.1029/JZ067i009p03627>, 1962.
- Skamarock, W. C., Klemp, J. B., Dudhia, J., Gill, D. O., Barker, D. M., Duda, K., Huang, X.-Y., Wang, W., and Powers, J. G.: A description of the advanced research WRF version 3, Tech. rep., DTIC Document, 2008.
- 20 Thayer, G. D.: An improved equation for the radio refractive index of air, *Radio Science*, 9, 803–807, 1974.
- Tomassini, M., Gendt, G., Dick, G., Ramatschi, M., and Schraff, C.: Monitoring of integrated water vapor from ground-based GPS observations and their assimilation in a limited-area model, *Phys. and Chem. of the Earth*, 27, 341–346, 2002.
- Tuller, S. E.: The world distribution of annual precipitation efficiency, *Journal of Geography*, 70, 219–223, 1971.
- 25 Van Malderen, R., Brenot, H., Pottiaux, E., Beirle, S., Hermans, C., De Mazière, M., Wagner, T., De Backer, H., and Bruyninx, C.: A multi-site intercomparison of integrated water vapour observations for climate change analysis, *Atmospheric Measurement Techniques*, 7, 2487–2512, doi:10.5194/amt-7-2487-2014, <http://www.atmos-meas-tech.net/7/2487/2014/>, 2014.
- Wilgan, K., Hurter, F., Geiger, A., Rohm, W., and Bosy, J.: Tropospheric refractivity and zenith path delays from least-squares collocation of meteorological and GNSS data, *Journal of Geodesy*, pp. 1–18, 2016.
- 30 Yuan, Y., Zhang, K., Rohm, W., Choy, S., Norman, R., and Wang, C. S.: Real-time retrieval of precipitable water vapor from GPS precise point positioning, *J. Geophys. Res.*, 119, 10 044–10 057, doi:10.1002/2014JD021486, 2014.
- Zumberge, J. F., Heflin, M. B., Jefferson, D. C., Watkins, M. M., and Webb, F. H.: Precise Point Positioning for the efficient and robust analysis of GPS data from large networks, *J. Geophys. Res.*, 102/3, 5005–5017, 1997.

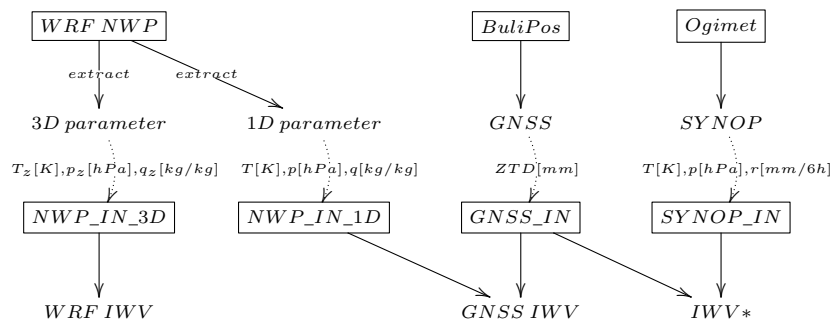


Figure 1. SUADA data flow.

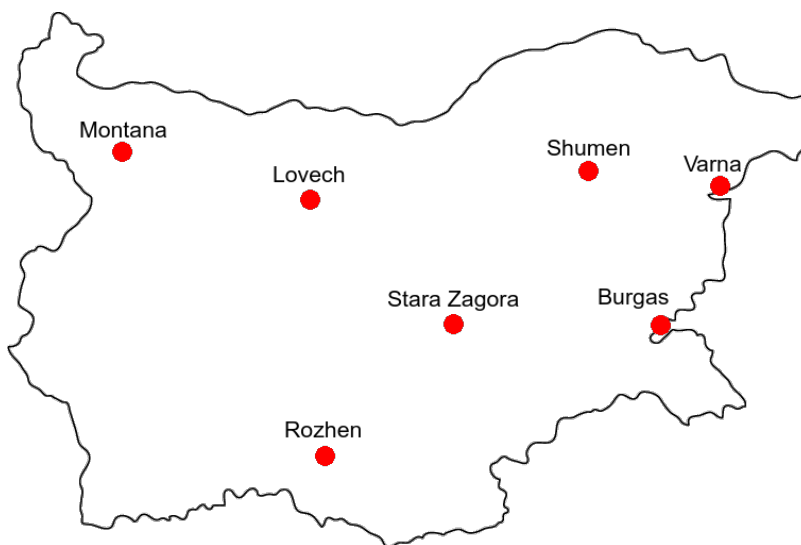


Figure 2. Map of the ground based stations of the BuliPos GNSS network. The red markers show the station locations.

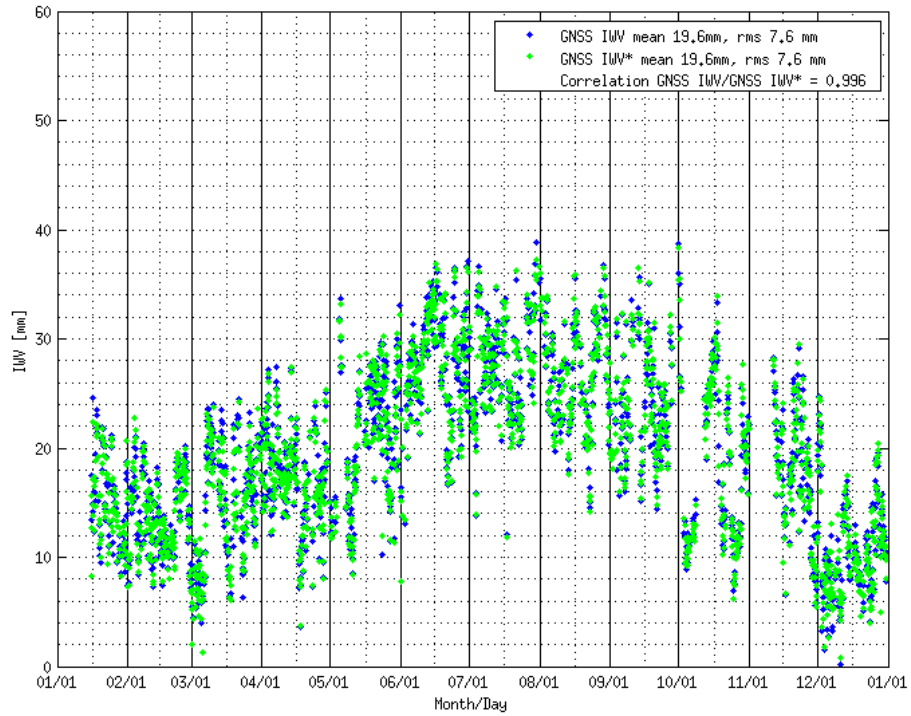
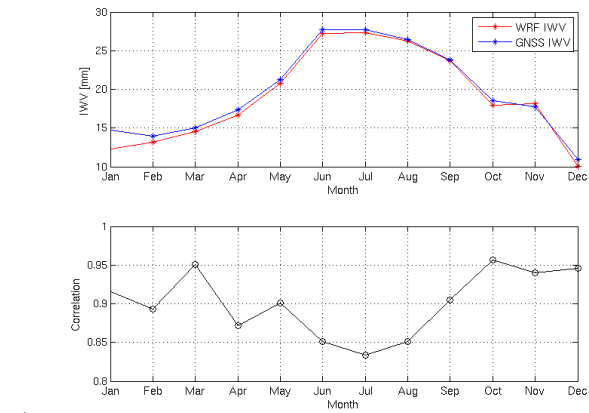


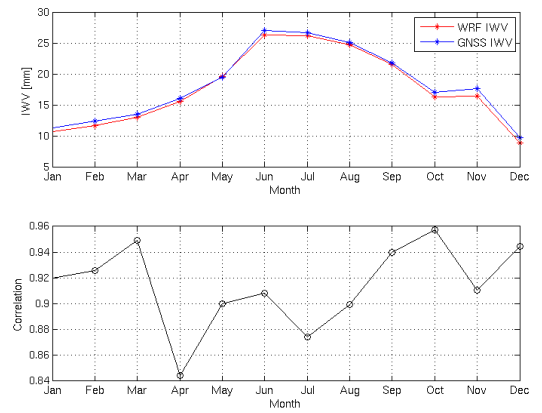
Figure 3. GNSS IWV and IWV* for station Burgas in 2013.

Station	Pressure WRF mean	Pressure SYNOP mean	Pressure WRF STD	Pressure SYNOP STD	Correlation coefficient
Lovech	1015.4	1015.9	7.4	7.4	0.989
Burgas	1015.6	1015.8	7.3	7.4	0.995
Varna	1015.6	1015.8	7.2	7.4	0.996
Station	Temperature WRF mean	Temperature SYNOP mean	Temperature WRF STD	Temperature SYNOP STD	Correlation coefficient
Lovech	15.1	14.0	8.7	9.6	0.957
Burgas	13.9	14.2	8.3	8.3	0.960
Varna	13.7	13.9	8.1	8.3	0.975
Station	GNSS IWV mean	IWV* mean	GNSS IWV STD	IWV* STD	Correlation coefficient
Lovech	18.2	17.0	7.6	7.3	0.999
Burgas	19.6	19.6	7.6	7.6	0.996
Varna	17.4	17.3	6.9	7.0	0.999

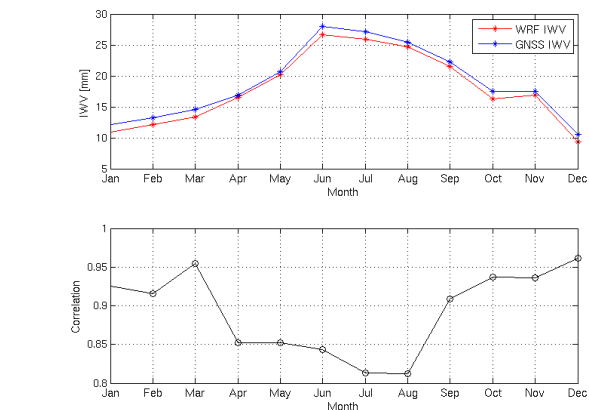
Table 1. Surface pressure (top) and temperature (middle) and IWV (bottom) from SYNOP and WRF. Mean (column 2 and 3), standard deviation (column 4 and 5) and correlation coefficient (column 6).



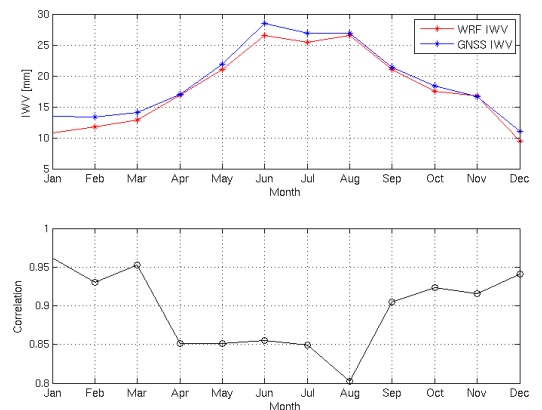
a)



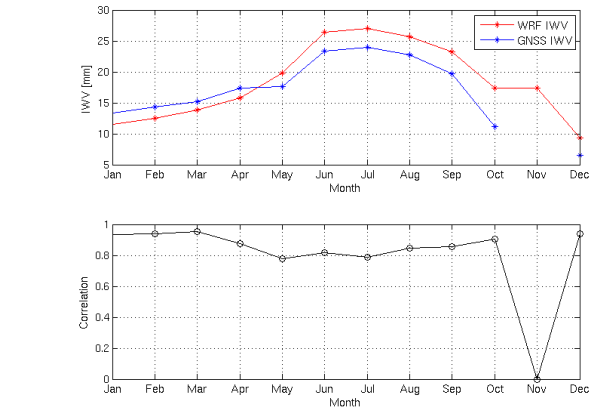
b)



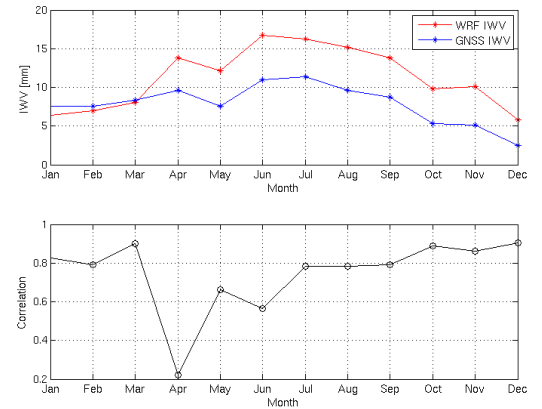
c)



d)



e)



f)

Figure 4. Top plots: IWV monthly mean from GNSS and WRF for: a) Burgas, b) Shumen, c) Stara Zagora, d) Montana, e) Varna and f) Rozhen in 2013. Bottom plots: correlation coefficient.

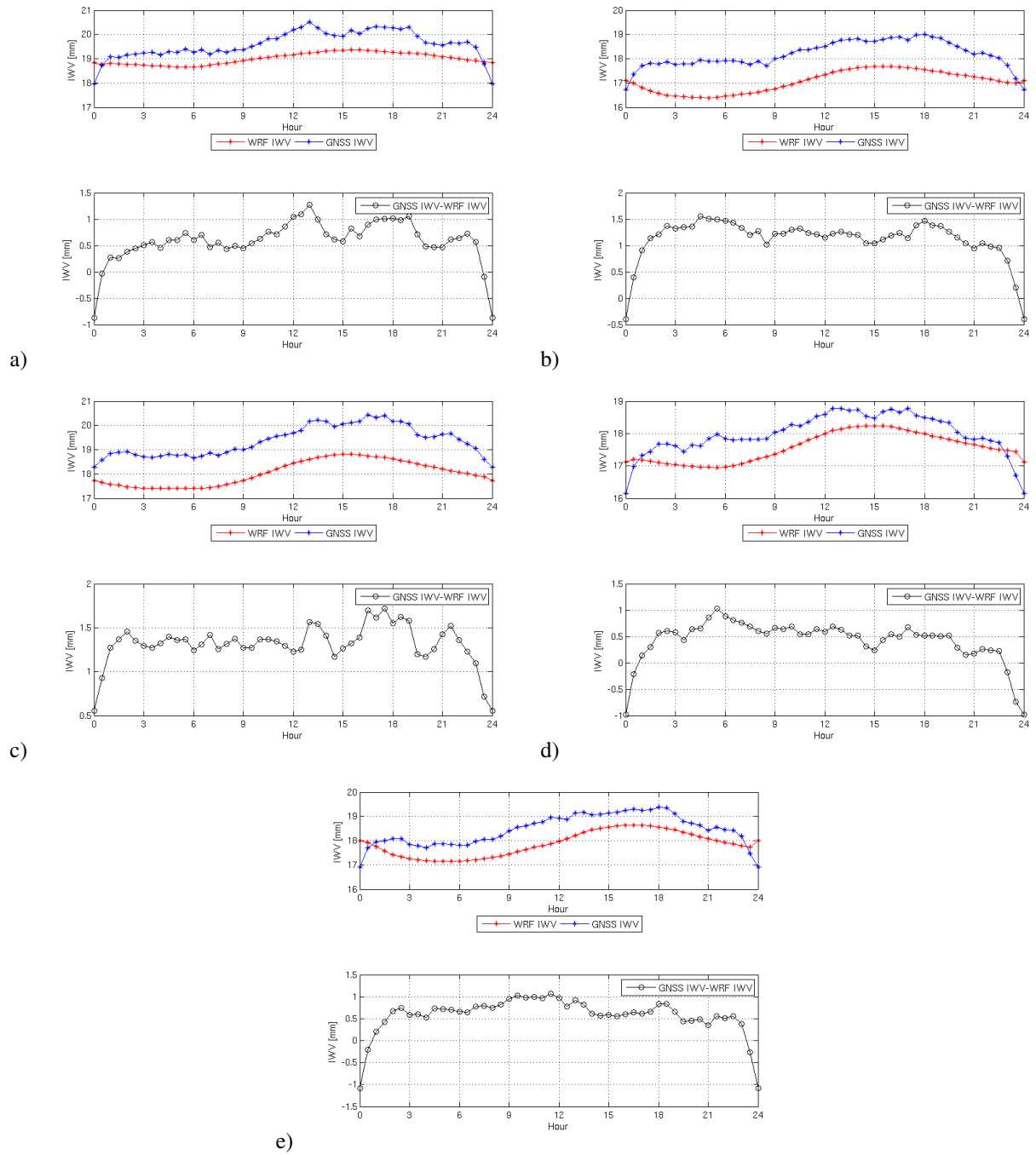
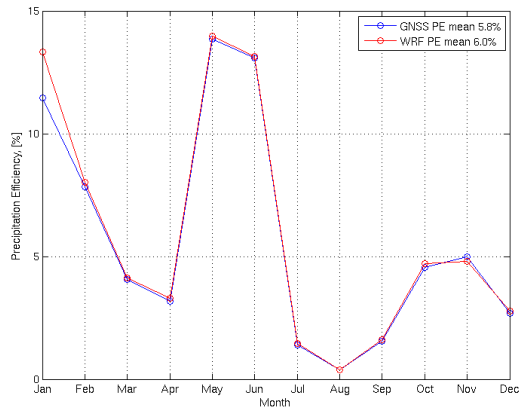
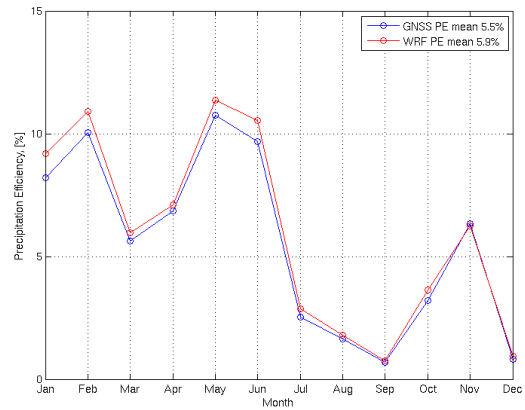


Figure 5. Top plots: IWV diurnal cycle from GNSS and WRF for: a) Burgas, b) Lovech, c) Montana, d) Shumen and e) Stara Zagora. Bottom plots: IWV difference GNSS minus WRF.

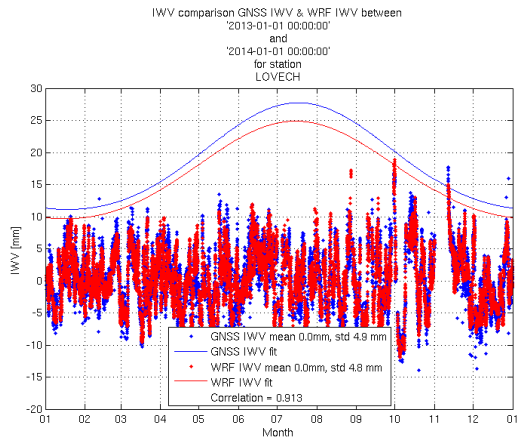


a)

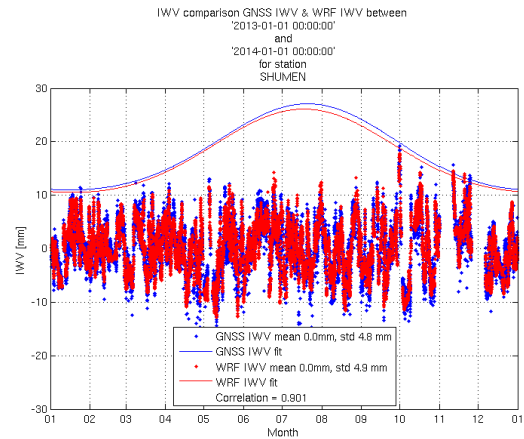


b)

Figure 6. Precipitation efficiency from GNSS and WRF for: a) Burgas and b) Lovech.



a)



b)

Figure 7. Detrended annual IWV variation from GNSS and WRF with annual fits for: a) Lovech and b) Shumen.

Station	GNSS elevation [m]	WRF level elevation [m]	SYNOP elevation [m]	GNSS-WRF diff [m]
Burgas	71	34	28	+66
Stara Zagora	227	254	-	-27
Shumen	268	243	-	+25
Montana	203	225	-	-22
Lovech	243	350	221	-107
Varna	62	96	43	-34
Rozhen	1779	1431	-	+348

Table 2. GNSS and meteorological stations and WRF surface level elevations

Station	GNSS IWV mean	GNSS IWV STD	WRF IWV mean	WRF IWV STD	GNSS/WRF IWV correlation	GNSS-WRF IWV mean difference
Montana	19.4	7.6	17.9	7.3	0.95	1.5
Lovech	18.2	7.6	16.4	7.2	0.96	1.8
Shumen	18.0	7.5	17.5	7.5	0.96	0.5
Burgas	19.6	7.6	19.0	7.6	0.96	0.6
Stara Zagora	18.5	7.5	17.3	7.4	0.96	1.2
Varna	17.4	6.9	18.3	7.9	0.90	-0.9
Rozhen	7.9	4.2	11.1	5.3	0.76	-3.2

Table 3. Mean (column 2 and 4), standard deviation (STD, column 3 and 5), correlation coefficient (column 6) and mean difference (column 7) of GNSS and WRF IWV for 2013.